e-Polymers **2008**, no. 076

http://www.e-polymers.org

ISSN 1618-7229

Crystalline form transformation of isotactic polypropylene induced by N,N'-diphenyl glutaramide

Quliang Lu, Qiang Dou[*]

[*]Department of Polymer Science, College of Materials Science and Engineering, Nanjing University of Technology, Nanjing, 210009, People's Republic of China; tel: 0086 25 83587264; fax: 0086 25 83240205; e-mail: douqiang.njut@163.com

(Received: 17 January, 2008; published: 15 June, 2008)

Abstract: N,N'-Diphenyl glutaramide (DPG) is found to be an effective nucleating agent to induce the β-form of iPP. The results of wide angle X-ray diffraction, differential scanning calorimetry and polarized light microscopy indicate that 0.2 wt% of DPG can induce the maximum amount of β-form iPP, and the favorable crystallization temperature for the growth of β-form is 120 ˚C in this study. Analysis of the misfit factor between the cell parameters of DPG and β-iPP shows β-iPP can epitaxially crystallize on the *bc* face of DPG crystal well.

Keywords: polypropylene; β crystalline form; N,N'-diphenyl glutaramide; nucleating agent; crystallization

Introduction

As a general-purpose plastic, isotactic polypropylene (iPP) has been widely used in many fields. The performance of material based on iPP resin depends strongly on its crystalline form and the degree of crystallinity. IPP has four kinds of crystalline forms: α, β, γ and smectic [1, 2]. α-form is the most common crystalline form and the γ-form shows the most thermodynamical stability [3-5]. In comparing with other three forms of iPP, β form iPP is a metastable one, but presents outstanding toughness, which has been applied in the industrial field to improve the impact strength of the iPP materials [6, 7]. The literatures [8, 9] reported rich β-form can exist in the iPP sample in the presence of specific nucleating agents. The first efficient nucleating agent was the γ-form of linear trans-quinacridone which was found by Leugering et al. [10]. But drawbacks such as intense red color and polymorphic nature are also very obvious, and limit the application. Some other β-form promoters such as calcium pimelate [11-13], N,N,N',N',-tetraalkyl terephthalamide [14], N,N'-dicyclohexyl-2,6-naphthalenedicarboxamide [15, 16], N,N'-dicyclo hexylterephthalamide [17], dicyclohexyl-substituted-1,4-phenylenebisamides [18], also have been found as effective β-nucleating agents for iPP.

The epitaxial crystallization mechanism has been widely used to explain the addition of nucleating agents in bulk semi-crystalline polymers. Traditionally, epitaxy is associated with dimensional matching rules between the contact planes of the interacting species. A long accepted rule of thumb is that oriented overgrowth requires a mismatch smaller than ± 15%. Large mismatches cannot be accommodated over large distances and will force the formation of dislocations or defects hence the disorientation of the deposit [19, 20]. The misfit factor (f_m) between the two crystal structures of iPP and the nucleating agent can be calculated

as $f_m = 100 \times \frac{PB - PA}{PA}$, in which PA and PB are the appropriate period length of substrate and polymer respectively [21]. In the present article, an organic compound (N,N'-diphenyl glutaramide) was synthesized and blended with iPP to induce the β-form of iPP. The influence of the content of the nucleating agent and the crystallization temperature on the β-form of iPP has been investigated.

Results and discussion

WAXD measurement

The WAXD patterns illustrate the influence of the content of DPG on the proportion of β-form iPP, as shown in Figure1. It can be found that when the content of DPG increases from 0.05% to 0.2%, the diffraction peak at 2θ = 16.2˚ increases, but those at 2θ =14.2°, 17° and 18.6° decline. The maximum percentage of β-form within the iPP is 86.12% when the content of DPG is 0.2% (see Table 1).

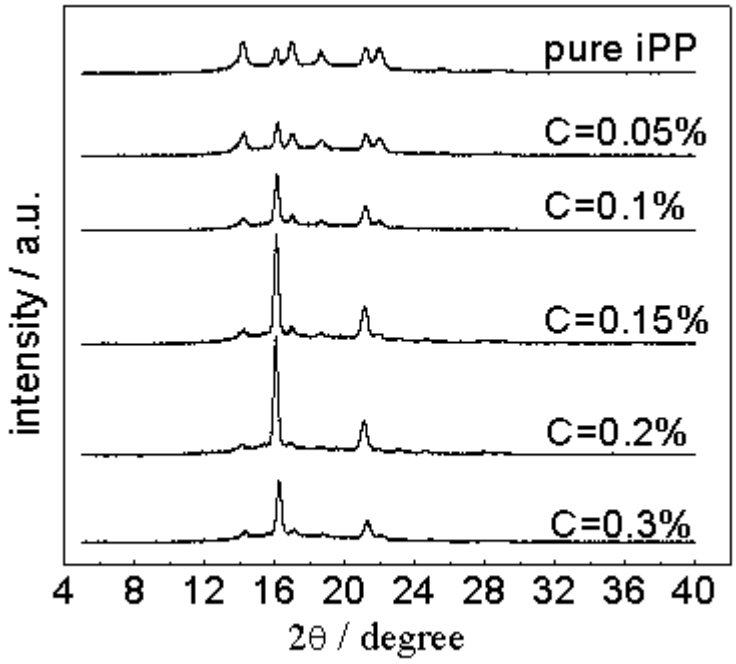

Fig. 1. WAXD patterns of iPP specimens doped with different content of DPG crystallized at 120 ˚C.

Tab. 1. Effect of DPG content on K_{WAXD} and X_{WAXD} of iPP samples crystallized at 120 ˚C.

DPG content (%)	0	0.05	0.1	0.15	0.2	0.3
K_{WAXD} (%)	21.2	38.2	79.6	82.8	86.1	75.2
X_{WAXD} (%)	50.5	53.9	62.5	65.0	71.7	60.8

The data listed in Table 1 also shows that the degree of crystallinity of samples increases with the increasing DPG content, which shows that more nucleating centres improve the proportion of crystalline phase. But when the content of DPG continues to increase (C=0.3%), the percentage of β-form and the degree of crystallinity decline. The phenomena maybe resulted from the superfluous DPG, which aggregates within the iPP resin, destroying the order of macromolecular chains, i.e. less chain is packed in the β-form lattice.

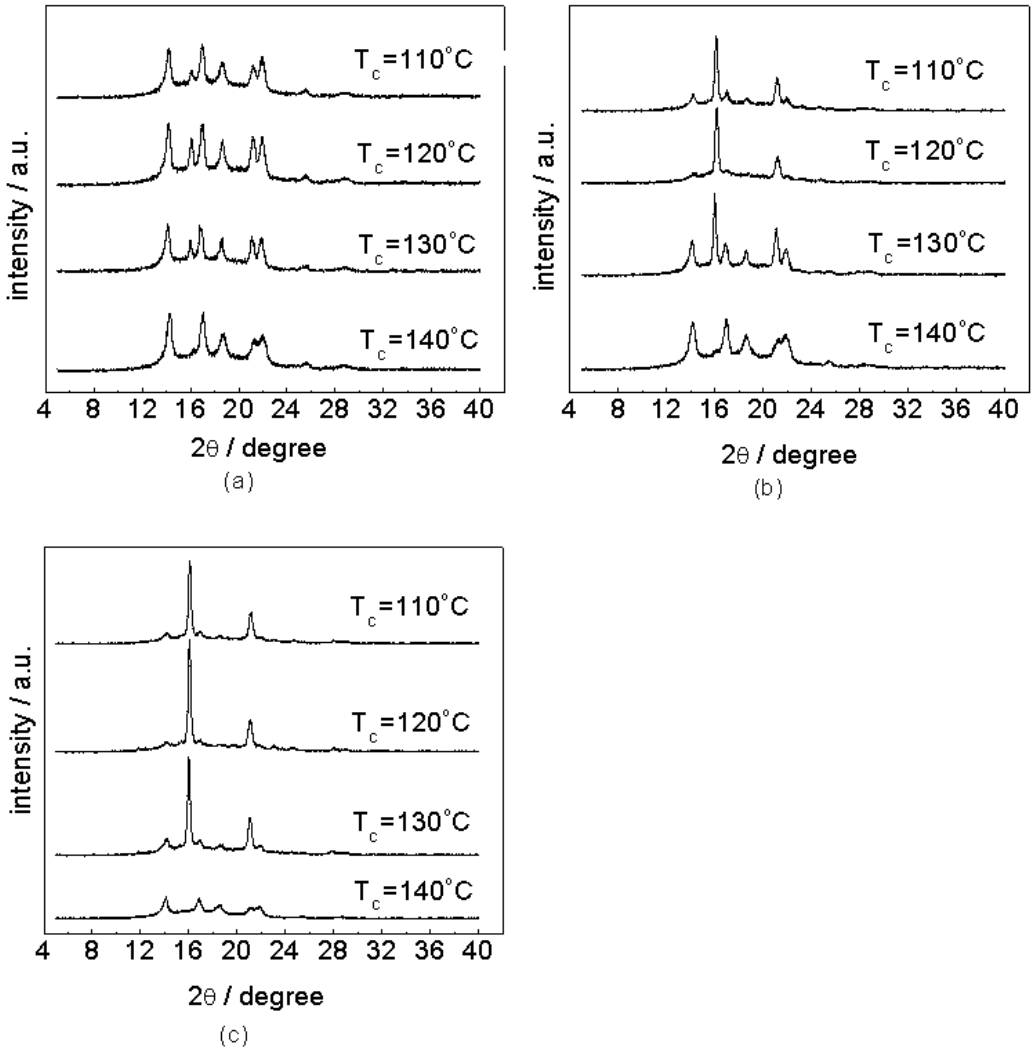

Fig. 2. WAXD patterns of iPP specimens doped with different contents of DPG crystallized at different crystallization temperatures.(a): pure iPP; (b): C=0.1%; (c): C=0.2%.

The suitable temperature range for the growth of β-form iPP is between 105 ˚C and 140 ˚C [22, 23]. We chose four crystallization temperatures (T_C) within the temperature range to study the effect of the T_C on the proportion of β-form and the degree of crystallinity, and to find the favorable T_C for the growth of β-form. As found in Table 2, the data unambiguously shows that the K_{WAXD} increases when T_C increases from 110˚C to 120˚C, then it decreases at higher T_C. When T_C is 140 ˚C, there only exists little proportion of β-form, especially for samples containing 0.2% DPG. These results clearly indicate that the β-form iPP is favored at 120 ˚C in

comparing with other three temperatures in this study. And when the sample crystallizes at 140 ˚C, the low content of β-form maybe result from its slow growth rate, and the fact that perfect crystal needs more time to form.

On the contrary, T_C does not show obvious influence on the degree of crystallinity (X_{WAXD}) when T_C increases from 110 ˚C to 130 ˚C. But the X_{WAXD} of all samples decrease when T_C increases to 140 ˚C, especially for sample containing 0.2% DPG. It can be concluded that at high T_C, high content of DPG does not improve the content of crystalline phase of iPP.

Tab. 2. The influence of DPG contents and crystallization temperatures on the K_{WAXD} and X_{WAXD}.

DPG content (%)	0		0.1		0.2	
T_C (˚C)	K_{WAXD} (%)	X_{WAXD} (%)	K_{WAXD} (%)	X_{WAXD} (%)	K_{WAXD} (%)	X_{WAXD} (%)
110	10.2	53.6	69.1	62.6	81.7	70.1
120	21.2	53.9	79.6	62.5	86.1	71.7
130	18.6	55.5	52.7	62.7	78.9	70.8
140	5.6	53.1	5.6	55.4	0	51.5

DSC measurement

The melting process of iPP samples is complex, the difference between the α-form and β-form can be revealed by DSC measurement. The melting curves of pure or nucleated iPP samples, which were treated under isothermal crystallization process, exhibit two melting peaks.

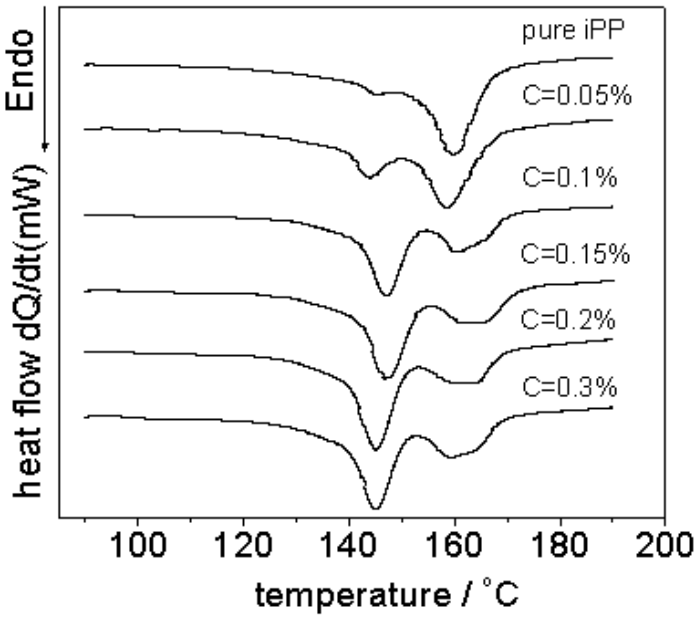

Fig. 3. Effect of the DPG contents on the DSC melting traces of β-nucleated iPP at the heating rate of 10 ˚C/min. All samples crystallized at 120 ˚C for 30 min.

Tab. 3. The quantitative results of the β-nucleated samples calculated from the DSC curves of Fig. 3.

DPG content (%)	$T_{m,\alpha}$ (˚C)	H_α (J/g)	$T_{m,\beta}$ (˚C)	H_β (J/g)	K_{DSC} (%)
0	161.5	108.3	146.9	21.2	15.7
0.05	160.6	94.6	145.6	44.0	30.7
0.1	163.1	53.1	148.7	75.6	57.5
0.15	164.5	43.1	148.6	75.9	62.6
0.2	165.6	45.2	146.9	89.5	65.3
0.3	161.2	47.9	146.7	73.7	59.4

Some literature [24-28] has reported that three phase transformations were inevitable while nucleated iPP sample undergoes heating process: the β-form melts; the new α-form recrystallizes from the original β-form and α-form melts finally. Figure 4 and Table 4 show the influence of heating rates on the melting curves of iPP samples. As can be observed, H_β increases with the increasing heating rate, but H_α shows an opposite changing trend. The observation indicates that under a slow heating rate condition, the β-form has more time to transform into the new α-form. But if the heating rate is fast, the β-form has less time to recrystallize into α-form. However, when the heating rate is 5 ˚C/min, three melting peaks can be found on the melting curve. Lots of literature [15, 29-31] has pointed out that the first two melting peaks correspond to β_1-form and β_2-form respectively, while the third one corresponds to α-form. The small intermediate β_2-form shows a more ordered and stable structure which recrystallizes from the original β_1-form.

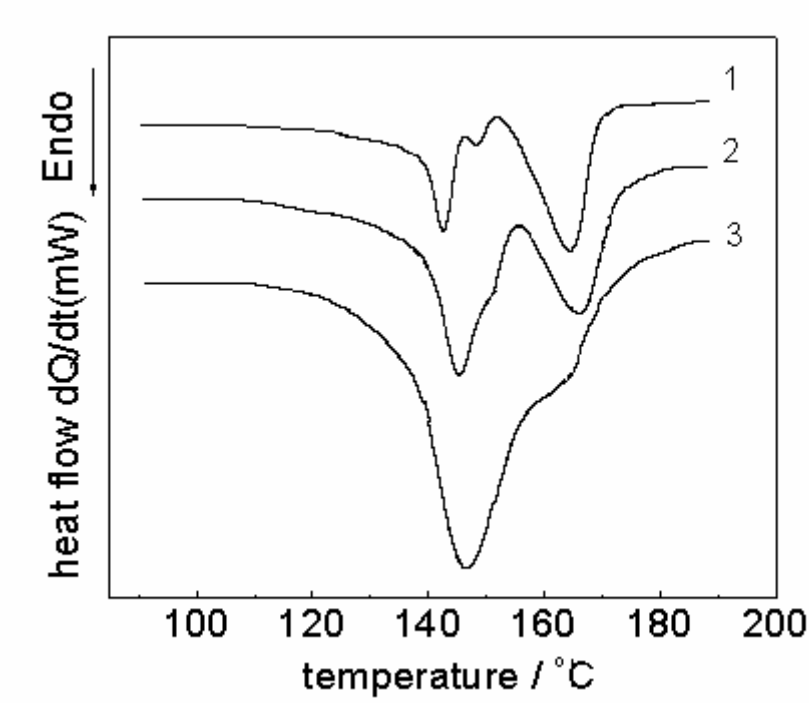

Fig. 4. DSC thermograms of nucleated iPP at different heating rates: (1) 5˚C/min; (2) 10˚C/min; (3) 20˚C/min. The DPG contents of the samples were 0.1%, and they were crystallized at 110˚C for 30mins. Heating rate is indicated on each curve.

Tab. 4. The quantitative results of the β-nucleated samples calculated from the DSC curves of Fig. 4.

Heating rate (˚C/min)	$T_{m,\alpha}$ (˚C)	H_α (J/g)	$T_{m,\beta}$ (˚C)	H_β (J/g)	K_{DSC} (%)
5	166.3	60.8	145.4 151.1	33.9	36.6
10	168.1	54.9	147.1	68.3	55.5
20	162.8	53.8	148.2	122.6	73.9

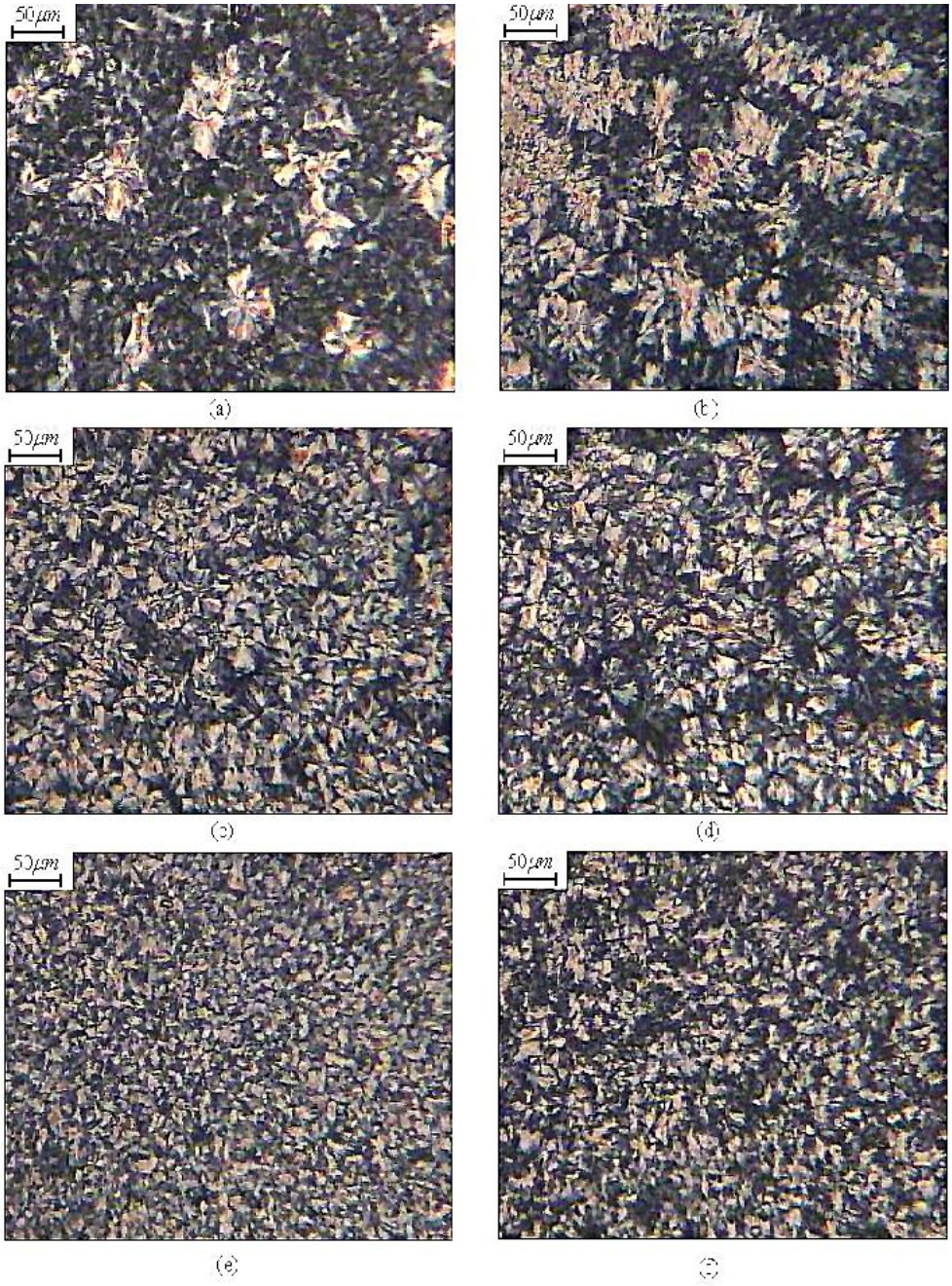

Fig. 5. The PLM images of iPP samples containing different contents of DPG. (a): pure iPP; (b): C=0.05%; (c): C=0.1%; (d): C=0.15%; (e): C=0.2%; (f): C=0.3%. All samples were crystallized at 120˚C for 30min.

PLM observation

The β-form of iPP exhibits bright and colored spherulitic structure in Figure 5. When the DPG content increases from 0% to 0.2%, the number of β-spherulites increases, and the size of the β-spherulites decreases. Because higher content of DPG provides more nucleating centres, which results in more numbers of β-spherulite. More nucleation centres promote the nucleation rate. The β-spherulite has less time to grow larger, which brings on smaller size of β-spherulite. But when the DPG content increases to 0.3%, the numbers of β-spherulites decreases somewhat (Figure 5f). This observation on the PLM images accords with the results of DSC and WAXD.

Analysis of the β nucleation mechanism of DPG

From the above discussion, we know that DPG is an active β nucleating agent for iPP. And when the molten iPP crystallized on the surface of DPG, the geometric relationship between the crystal of iPP and that of DPG should be considered. The main (and minimal) structural characteristics required for nucleating agents of β-iPP are the existence in the contact faces of a 0.65 nm periodicity which matches the iPP chain axis repeat distance and an orthogonal cell geometry in that contact plane [32, 33]. The diffraction pattern of DPG is shown in the Figure 6.

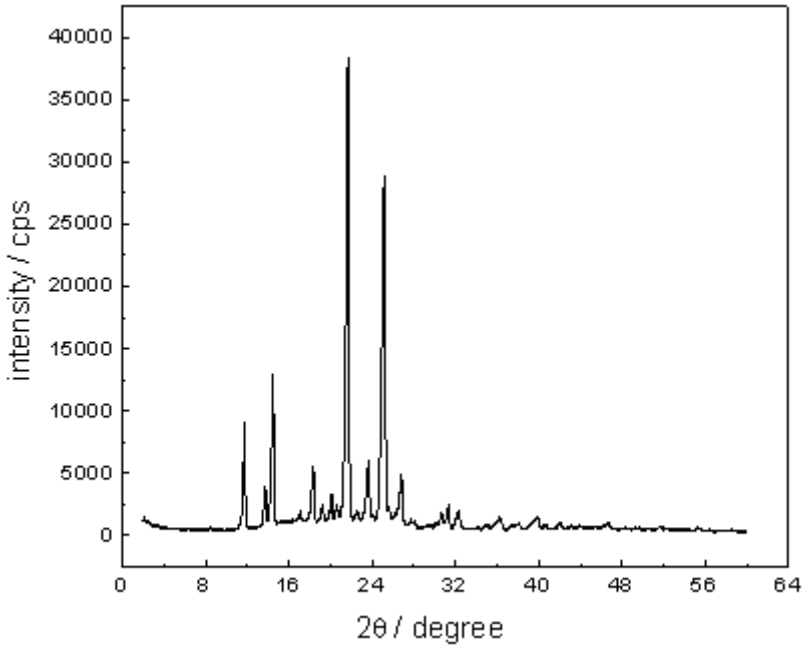

Fig. 6. The powder WAXD pattern of DPG.

The cell parameters of DPG which were calculated from the WAXD data, and those of β-iPP which were first revealed by Meille et al. [34], are summarized in Table 5. The misfit factaor f_m between the length of $c_{\beta\text{-iPP}}$ and that of b_{DPS} is about 6.9%, which shows a good matching relationship between them, and the c-axis of β-iPP is parallel with the b-axis of DPG. In addition, the misfit factor between the length of $b_{\beta\text{-iPP}}$ and that of c_{DPG} is 1.6%, which shows that one helical period of β-iPP can be packed in one span of the c-axis of DPG. Hence the molecular chains of iPP crystallized from the molten state deposit on the bc-face of DPG, which lines with benzene rings (see Fig. 7).

Tab. 5. The cell parameters of β-iPP and DPG.

	system	a (Å)	b (Å)	c (Å)	α (°)	β (°)	γ (°)
β-iPP	trigonal	11.03	11.03	6.49	90	90	60
DPG	triclinic	9.11	6.94	11.21	68.48	124.13	102.99

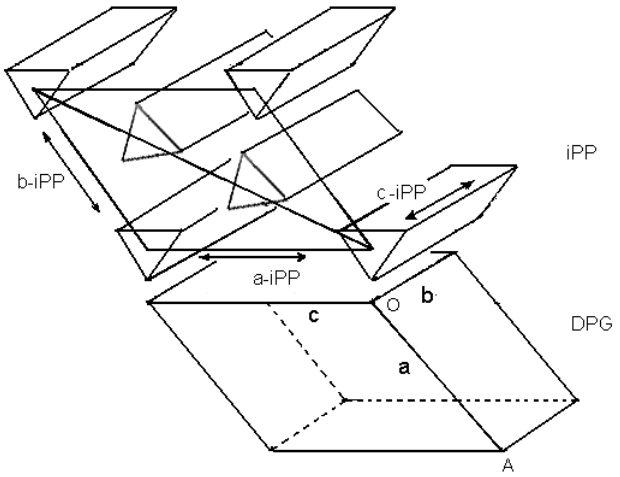

Fig. 7. The envisioned epitaxy of β-iPP crystal on the surface of DPG crystal.

Conclusions

In this study the organic compound N,N'-diphenyl glutaramide (DPG) was found as an effective β-nucleating agent for isotactic polypropylene. WAXD measurement reveals that DPG not only increase the degree of crystallinity of nucleated iPP, but also improve the formation of β-form. The percentage of β-form within the iPP sample reaches its maximum value with addition of 0.2 wt% DPG. And the favorable crystallization temperature for the growth of β-form is about 120 ˚C in this study. DSC measurement shows that H_β increases, but H_α declines with the increasing heating rate for the sample containg 0.1% DPG, which indicates that β-form has less time to transform into α-form due to higher heating rate. The size of β-spherulite can be reduced with the addition of DPG from the observation of PLM. The analysis of the cell parameters indicate that there exists excellent geometric matching between the crystal of DPG and that of β-form iPP.

Experimental part

Materials

IPP powder (MFR = 1 g/10 min at 230 ˚C and 21.2 N load) was obtained from Jingling Plastics and Rubber Chemical Co, Ltd. Industrial antioxidant (B215) was commercially available. N,N'-diphenyl glutaramide (DPG), which was synthesized in our laboratory, characterized by infrared technology (VECTORTM 22 Fourier transform infrared spectrometer, Bruker, Germeny) and ^{1}H NMR (AVANCE 400D+ HR/MAS, Bruker, Switzerland). The FTIR and ^{1}H NMR data of the DPG are given as below.

FTIR: 3310.94cm^{-1}($\upsilon_{\text{-NH}}$), 3080.78 cm^{-1} ($\upsilon\phi_{\text{-H}}$), 1745.15 cm^{-1} and 1673.18cm^{-1} ($\upsilon_{\text{C=O}}$), 1319.15 cm^{-1} and 1270.75 cm^{-1} ($\upsilon\phi_{\text{-N}}$), 1549.92 cm^{-1} and 1500.32 cm^{-1} ($\upsilon_{\text{-}}$

$_{CH}$). ^{1}H NMR (DMSO-d_6, 400MHz): δ=1.90ppm (m, 2H), δ=2.37ppm (t, 4H), δ=7.01ppm (t, 2H), δ=7.28ppm (t, 4H), δ=7.59ppm (d, 4H), δ=9.89ppm (s, 2H).

Preparation of nucleated iPP samples

200 g iPP powder was mixed with 0.2 g B215 and variable amounts of DPG in a mixer at the speed of 25000 rpm for 2 minutes. The mixtures were compounded in a single-screw extruder (LSJ20, D = 20 mm, L/D = 25/1, Shanghai KeChuang Rubber Plastic's Machinery Set Co. Ltd). The rate of the screw was 60 rpm. The temperature of the extruder from the hopper to the die was set at 210 ˚C, 220 ˚C, 220 ˚C and 210 ˚C, respectively. The melt was cooled and pelletized. IPP doped without DPG was prepared in a similar way to produce a blank control sample.

A pellet of the pure or nucleated iPP sample was placed between two glass slides on a hot stage kept at 210 ± 2 ˚C for 10 minutes to allow the sample to melt completely and remove thermal memory, squeezed on the top slide to form a film, and then put the specimens into glycerol bath at different temperature (110 ± 1˚C, 120 ± 1 ˚C, 130 ± 1 ˚C and 140 ± 1 ˚C respectively) to crystallize for 30 min, then quenched in ice water. The thickness of samples is ca. 0.5 mm for WAXD and DSC characterization and 20 ~ 40 μm for PLM observation, respectively.

Wide angle X-ray diffraction (WAXD) characterization

WAXD diffraction patterns of the nucleated iPP samples were recorded in an ARL X'TRA X-ray diffractometer (Thermo Electron Corporation, USA) using Cu Kα radiation (λ=1.54Å). It was operated at a voltage of 45 kV and a filament current of 35 mA. Radial scans of intensity vs. diffraction angle (2θ) were recorded in the range of 5 to 40˚, and the scanning rate was 10 ˚/min.

The characteristic crystal planes for the monoclinic α-phase of iPP are: (110), (040), (130) and (041) planes, which correspond to the diffraction angles 2θ=14.2°, 17°,18.6° and 22°, respectively. And the characteristic crystal planes (300) and (301) for β-form are characterized at the diffraction angles 2θ=16.2° and 21.2°. The relative proportion of β phase in the iPP specimen was measured by the empirical ratio K_{WAXD} [35]:

$$K_{WAXD} = \frac{H(300)}{H(300) + H(110) + H(040) + H(130)} \quad (1)$$

The H (300), H (110), H (040) and H (130) are the heights of the peaks of β-form (300) and three strong α-form peaks (110), (040) and (130), respectively. All the heights of the peaks were measured above the amorphous background. The total degree of crystallinity (X_{WAXD}) of the sample was calculated by the function as below:

$$X_{WAXD} = \frac{I_C}{I} \times 100 \quad (2)$$

where I_C was the integral intensities diffracted by a crystalline part, and I was the total integral intensities [36].

N,N'-diphenyl glutaramide was also investigated by the same X-ray diffractometer. The scanning angle range was 2 to 60˚, and the scanning rate was 2 ˚/min.

Differential scanning calorimetry (DSC) measurement

The thermal property of pure iPP and nucleated iPP were measured by a DSC instrument (CDR-34P, Shanghai Precision Scientific Instrument Co. Ltd) under a dry nitrogen atmosphere. For sample measurement, about 4 ~ 6 mg of each sample was sealed in an aluminium pan and heated from room temperature to 220 ˚C at a heating rate of 10 ˚C /min. The heat flow and the temperature were recorded. The peak melting temperatures of the α form ($T_{m,\alpha}$) and β form ($T_{m,\beta}$) were obtained from the melting curves. The enthalpy of the α-form (H_α) and β-form (H_β) were obtained from the separation of the areas of α- and β-form melting peaks. The content of β-form is calculated by the functions as below:

$$K_{DSC} = H_{m,\beta}/(H_{m,\beta} + H_{m,\alpha}) \quad (3)$$

where $H^0_{m,\alpha}$ is the enthalpy of α-form PP with 100% crystallinity (177.0J/g), and $H^0_{m,\beta}$ is the enthalpy of β-form PP with 100% crystallinity (168.5J/g) [37].

Polarized light microscopy (PLM) observation

Crystal morphology of the pure and nucleated iPP samples were observed by a polarized light microscope (LW-200-4JS, Shanghai LW Scientific Co. Ltd) equipped with cross polars and a CCD camera.

References

[1] Nedkov, E.; Dobreva T. *e-Polymers* **2002**, no. 042.
[2] Tjong, S. C.; Bao, S. *e-Polymers* **2007**, no.139.
[3] Dimeska, A.; Phillips, P. J. *Polymer* **2006**, *47*, 5445.
[4] Mezghani, K.; Phillips, P. J. *Polymer* **1997**, *38*, 5725.
[5] Mezghani, K.; Phillips, P. J. *Polymer* **1998**, *39*, 3735.
[6] Zhang, P.; Liu, X.; Li, Y. *Mat. Sci. Eng. A*. **2004**, *434*, 310.
[7] Martin, O.; Čermák, R.; Baran, N. *Int. Polym. Process.* **2004**, *19*, 35.
[8] Varga, J. *J. Mater. Sci.* **1992**, *27*, 2557.
[9] Zhou, J.-J.; Liu, J.-G.; Yan, S.-K.; Dong, J.-Y.; Li, L.; Chan, Ch-M.; Schultz J. M. *Polymer* **2005**, *46*, 4077.
[10] Leugering, V. H. J. *Makromol. Chem*. **1967**, *109*, 204.
[11] Dou, Q. *J. Macromol. Sci. Phys.* **2007**, *46*, 1063.
[12] Dou, Q. *J. Macromol. Sci. Phys.* **2008**, *47*, 127.
[13] Dou, Q. *J. Appl. Polym. Sci.* **2008**, *107*, 958.
[14] Shentu, B-q.; Li, J.; Weng, Z. *Chinese J. Polym. Sci*. **2006**, *24*, 345.
[15] Ščudla, J.; Raab, M.; Eichhorn, K-J.; Strachota, A. *Polymer* **2003**, *44*, 4655.
[16] Varga, J.; Menyhárd, A. *Macromolecules* **2007**, *40*, 2422.
[17] Zhang, Y. F.; Xin, Z. J*. Polym. Sci. Polym. Phys.* **2007**, *45*,590.
[18] Mohmeyer, N.; Schmidt, H-W.; Kristiansen P. M.; Altstadt, V. *Macromolecules* **2006**, *39*, 5760.
[19] Wittmann, J. C.; Lotz, B. *Prog. Polym. Sci.* **1990***, 15,* 909.
[20] Thierry, A.; Mathieu, C.; Straupe, C.; Wittmann, J. C.; Lotz, B. *Macromol. Symp.* **2001**, *166*, 43.
[21] Kawai, T.; Iijima, R.; Yamamoto, Y. ; Kimura, T. *Polymer* **2002**, *43*, 7301.
[22] Varga, J. *J. Macromol. Sci. Phys.* **2002**, *41*, 1121.
[23] Lotz, B. *Polymer* **1998**, *39*, 4561.

[24] Zhou G.; He, Z.; Yu, J. *Macromol. Chem.* **1986**, *187*, 633.
[25] Varga, J. *J. Therm. Anal. Cal*. **1986**, *31*, 165.
[26] Marigo, A.; Marega, C.; Causin, V.; Ferrari, P. *J. Appl. Polym. Sci*. **2004**, *91*, 1008.
[27] Quan, Y.; Jiang, W.; An, L. *Colloid Polym. Sci.* **2004**, *282*, 1236.
[28] Yamamoto, Y.; Inoue, Y.; Onai, T. ; Doshu, C.; Takahashi, H.; Uehara, H. *Macromolecules* **2007**, *40*, 2745.
[29] Ščudla, J.; Eichhorn, K-J.; Raab, M.; Schmidt, P.; Jehnichen, D.; Häuβler, L. *Macromol. Symp.* **2002**, *184*, 371.
[30] Cho, K.; Saheb, D. N.; Yang, H.; Kang, B-II.; Kim, J.; Lee, S-S. *Polymer* **2003**, *44*, 4053.
[31] Cho, K.; Saheb, D. N.; Choi, J.; Yang, H. *Polymer* **2002**, *43*, 1407.
[32] Mathieu, C.; Thierry, A.; Wittmann, J. C.; Lotz, B. *J. Polym. Sci. Polym. Phys.* **2002**, *40*, 2504.
[33] Stocker, W.; Schumacher, M.; Graff, S.; Thierry, A.; Wittmann, J. C.; Lotz, B. *Macromolecules* **1998**, *31*, 807.
[34] Meille, S. V.; Ferro, D. R.; Bruckner, S.; Lovinger, A. J.; Padden, F. J. *Macromolecules* **1994**, *27*, 2615.
[35] Turner-Jones, A.; Aizlewood, J. M.; Beckett, D. R. *Makromol. Chem.* **1964**, *75*, 134.
[36] Martin, O.; Roman, C.; Raab, M. .; Verney, V.; Commereuc, S.; FraÏsse, F. *Polym. Degrad. Stab.* **2005**, *88*, 532.
[37] Li, J. X.; Cheung, W. L.; Jia, D. *Polymer*. **1999**, *40*, 1219.